Molecular Biology of the Cell
Vol. 8, 1829–1844, October 1997

The Rho-GEF Rom2p Localizes to Sites of Polarized Cell Growth and Participates in Cytoskeletal Functions in *Saccharomyces cerevisiae*

Brendan D. Manning, Ramesh Padmanabha, and Michael Snyder*

Department of Biology, Yale University, New Haven, Connecticut 06520-8103

Submitted May 15, 1997; Accepted July 1, 1997
Monitoring Editor: W. James Nelson

Rom2p is a GDP/GTP exchange factor for Rho1p and Rho2p GTPases; Rho proteins have been implicated in control of actin cytoskeletal rearrangements. *ROM2* and *RHO2* were identified in a screen for high-copy number suppressors of *cik1*Δ, a mutant defective in microtubule-based processes in *Saccharomyces cerevisiae*. A Rom2p::3XHA fusion protein localizes to sites of polarized cell growth, including incipient bud sites, tips of small buds, and tips of mating projections. Disruption of *ROM2* results in temperature-sensitive growth defects at 11°C and 37°C. *rom2*Δ cells exhibit morphological defects. At permissive temperatures, *rom2*Δ cells often form elongated buds and fail to form normal mating projections after exposure to pheromone; at the restrictive temperature, small budded cells accumulate. High-copy number plasmids containing either *ROM2* or *RHO2* suppress the temperature-sensitive growth defects of *cik1*Δ and *kar3*Δ strains. *KAR3* encodes a kinesin-related protein that interacts with Cik1p. Furthermore, *rom2*Δ strains exhibit increased sensitivity to the microtubule depolymerizing drug benomyl. These results suggest a role for Rom2p in both polarized morphogenesis and functions of the microtubule cytoskeleton.

INTRODUCTION

The cytoskeleton is the infrastructure of the cell; it aids in determining cell shape and participates in many dynamic cellular processes. Two major components of all eukaryotic cytoskeletons are microfilaments, composed of actin subunits, and microtubules, made up of tubulin heterodimers. The two systems are involved in distinct processes within the cell. This is particularly evident in the budding yeast *Saccharomyces cerevisiae*. The primary functions of the yeast actin cytoskeleton are in secretion, cell growth and polarized morphogenesis, resulting in bud and mating projection formation (Adams and Pringle, 1984; Kilmartin and Adams, 1984; Novick and Botstein, 1985; Read *et al.*, 1992). Yeast microtubules are dispensable for secretion and cell growth; instead, they are required for nuclear positioning, chromosome segregation during mitosis and meiosis, and nuclear fusion during mating (karyogamy; Adams and Pringle, 1984; Kilmartin and Adams, 1984; Huffaker *et al.*, 1988; Jacobs *et al.*, 1988; Snyder *et al.*, 1991; reviewed in Page and Snyder, 1993).

Studies of the regulation of cytoskeletal function and rearrangement in a wide variety of eukaryotes have provided insight into the mechanisms controlling the organization of microfilaments and, to a lesser degree, microtubules. A family of highly conserved ras-homologous small GTPases, known as Rho proteins, have emerged as key molecular switches that regulate organization of the actin cytoskeleton (reviewed in Hall, 1994; Ridley, 1995).

Rho proteins cycle between a GTP-bound active state and a GDP-bound inactive state with the assistance of several important classes of regulatory proteins. One type of Rho regulator is the GDP/GTP-exchange factor (GEF), which stimulates release of GDP from the Rho protein, allowing subsequent binding of GTP and thereby Rho activation (Hart *et al.*, 1991). The Rho protein is returned to the GDP-bound inactive state by a Rho-specific GTPase-activating pro-

* Corresponding author: Department of Biology, P.O. Box 208103, Yale University, New Haven, CT 06520-8103.

tein (GAP) that stimulates the inherent GTPase activity of the Rho protein (Ridley, 1995, and references therein). Additional Rho regulation involves Rho-GDP dissociation inhibitors that bind Rho proteins in their GDP-bound form and prevent exchange for GTP, thus locking them in the inactive state (Ohga *et al.*, 1989; Fukumoto *et al.*, 1990).

Five genes encoding members of the Rho family have been identified in *S. cerevisiae*, including *CDC42*, *RHO1*, *RHO2*, *RHO3*, and *RHO4*. All have been implicated in controlling polarized cell morphogenesis during bud and/or mating projection formation (Madaule *et al.*, 1987; Adams *et al.*, 1990; Johnson and Pringle, 1990; Matsui and Toh-e, 1992; Li *et al.*, 1995; Imai *et al.*, 1996). Cdc42p and Rho1p are essential and localize to sites of polarized cell growth, which are regions where actin patches accumulate (Ziman *et al.*, 1993; Yamochi *et al.*, 1994). Rho1p has recently been shown to regulate both cell wall biosynthesis and protein kinase C (Pkc1p) signaling (Drgonova *et al.*, 1996; Qadota *et al.*, 1996).

Members of the different classes of Rho regulators have also been identified in *S. cerevisiae. CDC24* encodes a GEF for Cdc42p, and *ROM1* and *ROM2* encode GEFs for Rho1p (Zheng *et al.*, 1994; Ozaki *et al.*, 1996; Schmidt *et al.*, 1997). *BEM3* encodes a GAP for Cdc42p, and *BEM2* and *SAC7* encode GAPs for Rho1p (Zheng *et al.*, 1993; Peterson *et al.*, 1994; Schmidt *et al.*, 1997). Genetic evidence suggests that Rom2p and Bem2p also regulate Rho2p activity (Kim *et al.*, 1994; Ozaki *et al.*, 1996; Schmidt *et al.*, 1997; this study). Finally, a Rho-GDP dissociation inhibitor that binds Rho1p is encoded by *RDI1* (Masuda *et al.*, 1994).

Although the biochemical functions of Rho regulators have been well-characterized in both yeast and mammalian cells, much less is known about their cellular distribution and how they are controlled. The only direct Rho regulator whose subcellular distribution has been determined is *S. cerevisiae* Cdc24p, which localizes over the entire cell periphery (Pringle *et al.*, 1995). This pattern contrasts that of the Cdc24p target Cdc42p, which concentrates at sites of polarized cell growth (Ziman *et al.*, 1993). Whether other regulators localize and function at sites of Rho protein activity is an important but unresolved issue.

We have identified *ROM2* in a screen for high-copy suppressors of *cik1*Δ, a mutant defective in microtubule-based processes (Page and Snyder, 1992). During the course of our work, *ROM2* was also identified by two other groups, as a high-copy suppressor of both a cold-sensitive *rho1* strain (Ozaki *et al.*, 1996) and a temperature-sensitive *tor2* strain (Schmidt *et al.*, 1997). *TOR2* encodes a phosphatidylinositol kinase homologue required for initiation of translation in response to nutrient concentrations (Barbet *et al.*, 1996; DiComo and Arndt, 1996) and is also involved in polarization of the actin cytoskeleton (Schmidt *et al.*, 1996). To further elucidate the function of *ROM2*, we localized its protein product and analyzed the phenotypes resulting from a *rom2* null mutation. Our findings demonstrate that Rom2p is concentrated at sites of polarized growth in a cell-cycle–dependent manner, the first such localization for a regulator of Rho proteins. Phenotypic and genetic analysis suggests that Rom2p is involved in both cell morphogenesis and microtubule function. Possible mechanisms for such roles are discussed.

MATERIALS AND METHODS

Yeast Strains, Media, and Standard Methods

Yeast strains used in this study are listed in Table 1. Yeast genetic methods and growth media were as described in Guthrie and Fink (1991). Rich medium consisted of yeast extract, peptone, and dextrose, supplemented with adenine (YPDA). Yeast transformations were by the lithium acetate method of Ito *et al.* (1983). Where indicated, benomyl (DuPont, Wilmington, DE) dissolved in dimethyl sulfoxide was added to YPDA medium to final concentrations of 10, 20, and 30 μg/ml. For the *ROM2* overexpression experiments, cells containing YEp24-*ROM2* or YEp24 plasmids were first grown on SC medium lacking uracil prior to incubation on benomyl plates; this increases the benomyl sensitivity of these strains relative to those grown initially in YPDA medium.

Construction of Epitope-tagged Rom2p Strains

A strain containing the *ROM2::3XHA* allele (Y1722) was constructed by using the polymerase chain reaction (PCR) epitope-tagging method of Schneider *et al.* (1995). The primers 5′-GCTACGAGGATTATCGCGGGTATGATACAGTTGCGTCGTTAGATTTCTGGGGTAGGGAACAAAAGCTGG-3′ and 5′-GCTTTTTTATTCTAAAGAAAATAAGGAAAGTCTATATACGTTGCTATCCTATAGGGCGAATTGG-3′ were used to amplify an ~1.5-kb region of pMPY-3xHA. The PCR product contains the *URA3* gene flanked by direct repeats encoding three copies of the hemagglutinin (HA) epitope and contains 53 bp of sequence from the 3′ end of the *ROM2* gene at one end and the *ROM2* translation termination codon and 45 bp of downstream sequence at the other end. This DNA fragment was used to transform yeast strain Y1721; transformants were selected on synthetic complete medium lacking uracil. For three strains, PCR analysis confirmed correct integration immediately upstream of the *ROM2* stop codon. These strains were incubated on plates containing medium with 5-fluoroorotic acid to select for cells that had lost the *URA3* gene through recombination between the two 3XHA coding regions. This event, as confirmed by PCR and immunoblot analysis, leaves a single in-frame copy of the 3XHA-encoding sequence at the carboxyl-terminal coding end of the *ROM2* gene.

Yeast Immunoblot Analysis

Cells were grown in 10 ml of YPDA to early-logarithmic phase (OD_{600} = 0.5) and washed, and pellets were frozen at −70°C for 2 h. After thawing on ice, cells were lysed by using glass beads in 100 μl of lysis buffer (1% Nonidet P-40, 0.5% sodium deoxycholate, 0.1% SDS, 150 mM NaCl, 50 mM Tris(hydroxymethyl)aminomethane hydrochloride, pH 7.5) containing protease inhibitors (1 mM phenylmethylsulfonyl fluoride, 1 μg/ml leupeptin, 1 μg/ml pepstatin, 10 μg/ml soybean trypsin inhibitor, and 10 μg/ml L-1-tosylamide-2-phenylethyl chloromethyl ketone). Lysates were centrifuged for 10 min at 14,000 × *g* to remove unlysed cells and cell debris. Cell lysates were then mixed at a 4:1 (vol/vol) ratio with fivefold-concentrated Laemmli sample buffer (Sambrook *et al.*, 1989) and boiled for 5 min before loading onto 8% polyacrylamide gels con-

Table 1. Strain list

Strain	Genotype
Y270	*MAT***a**/*MATα ura3-52/ura3-52 lys2-801/lys2-801 ade2-101/ade2-101 trp1-Δ1/trp1-Δ1 his3-Δ200/his3-Δ200*
Y930	*MAT***a** *ura3-52 lys2-801 ade2-101 trp1-Δ1 his3-Δ200 bem2Δ::URA3*
Y1241	*MAT***a**/*MATα ura3-52/ura3-52 lys2-801/lys2-801 ade2-101/ade2-101 trp1-Δ1/trp1-Δ1 his3-Δ200/his3-Δ200 rom2Δ::HIS3/ROM2*
Y1242	*MATα ura3-52 lys2-801 ade2-101 trp1-Δ1 his3-Δ200 rom2Δ::HIS3*
Y1243	*MATα ura3-52 lys2-801 ade2-101 trp1-Δ1 his3-Δ200*
Y1244	*MAT***a** *ura3-52 lys2-801 ade2-101 trp1-Δ1 his3-Δ200*
Y1245	*MAT***a** *ura3-52 lys2-801 ade2-101 trp1-Δ1 his3-Δ200 rom2Δ::HIS3*
Y1693	*MAT***a**/*MATα ura3-52/ura3-52 lys2-801/lys2-801 ade2-101/ade2-101 trp1-Δ1/trp1-Δ1 his3-Δ200/his3-Δ200 rho2Δ::TRP1/RHO2*
Y1695	*MAT***a** *ura3-52 lys2-801 ade2-101 trp1-Δ1 his3-Δ200 rho2Δ::TRP1*
Y1698	*MAT***a**/*MATα ura3-52/ura3-52 lys2-801/lys2-801 ade2-101/ade2-101 trp1-Δ1/trp1-Δ1 his3-Δ200/his3-Δ200 kar3Δ::TRP1/KAR3*
Y1700	*MAT***a** *ura3-52 lys2-801 ade2-101 trp1-Δ1 his3-Δ200 kar3Δ::TRP1*
Y1703	*MAT***a**/*MATα ura3-52/ura3-52 lys2-801/lys2-801 ade2-101/ade2-101 trp1-Δ1/trp1-Δ1 cik1Δ::TRP1/CIK1*
Y1705	*MAT***a** *ura3-52 lys2-801 ade2-101 trp1-Δ1 his3-Δ200 cik1Δ::TRP1*
Y1709[a]	*MAT***a**/*MATα ura3-52/ura3-52 lys2-801/lys2-801 ade2-101/ade2-101 trp1-Δ1/trp1-Δ1 his3-Δ200/his3-Δ200 bem2Δ::URA3/BEM2 rom2Δ::HIS3/ROM2*
Y1709-1	*MAT***a** *ura3-52 lys2-801 ade2-101 trp1-Δ1 his3-Δ200 bem2Δ::URA3 rom2Δ::HIS3*
Y1721	*MAT***a**/*MATα ura3-52/ura3-52 lys2-801/lys2-801 ade2-101/ade2-101 trp1-901/trp1-901 his3-Δ200/his3-Δ200 leu2-98/leu2-98*
Y1722	*MAT***a**/*MATα ura3-52/ura3-52 lys2-801/lys2-801 ade2-101/ade2-101 trp1-901/trp1-901 his3-Δ200/his3-Δ200 leu2-98/leu2-98 ROM2::3XHA/ROM2*
Y1723	*MATα ura3-52 lys2-801 ade2-101 trp1-901 his3-Δ200 leu2-98 ROM2::3XHA*
Y1724	*MAT***a** *ura3-52 lys2-801 ade2-101 trp1-901 his3-Δ200 leu2-98 ROM2::3XHA*
Y1725	*MATα ura3-52 lys2-801 ade2-101 trp1-901 his3-Δ200 leu2-98*
Y1726	*MAT***a** *ura3-52 lys2-801 ade2-101 trp1-901 his3-Δ200 leu2-98*
Y1727[b]	*MAT***a**/*MATα ura3-52/ura3-52 lys2-801/lys2-801 ade2-101/ade2-101 trp1-Δ1/trp1-Δ1 his3-Δ200/his3-Δ200 rom2Δ::HIS3/rom2Δ::HIS3*
Y1728	*MAT***a** *ura3-52 lys2-801 ade2-101 his3-Δ200 leu2-98 cik1Δ::LEU2*

[a] Y930 × Y1242.

[b] Y1242 × Y1245.

taining SDS. After electrophoretic separation, proteins were blotted onto Immobilon-P (Millipore, Bedford, MA) and probed with monoclonal anti-HA antibodies (12CA5 from BABCO, Richmond, CA); reactive bands were detected using alkaline phosphatase-conjugated anti-mouse antibodies (Ambersham, Arlington Heights, IL) and the CDP Star detection reagent (Boehringer Mannheim, Indianapolis, IN).

Fluorescence Microscopy

Indirect immunofluorescence was performed as described by Gehrung and Snyder (1990) and Pringle *et al.* (1991). Cells were fixed in 3.7% formaldehyde for 30 min, washed twice, and resuspended in 1.2 M sorbitol and 50 mM potassium phosphate buffer, pH 6.8 (solution A). Spheroplasts were prepared by incubating fixed cells in solution A containing 5 μg/ml Zymolyase 100T, 0.03% glusulase, and 0.2% 2-mercaptoethanol at 37°C for 30 min. Spheroplasts were washed, resuspended in solution A, and placed onto poly(L-lysine)-coated slides. Rom2p::3XHA was detected by primary antibody incubation overnight at 4°C with mouse 12CA5 antibodies diluted in 0.15 M NaCl, 0.05 M sodium phosphate, pH 7.4, and 0.1% bovine serum albumin (BSA; PBS/BSA), and secondary antibody incubation was for 2 h at room temperature with CY3-conjugated goat anti-mouse antibodies (Jackson ImmunoResearch, West Grove, PA) diluted in PBS/BSA. After both primary and secondary antibody incubations, slides were washed with PBS/BSA twice and PBS/BSA containing 0.1% Nonidet P-40 once. Finally, slides were mounted in 70% glycerol, 2% *n*-propyl gallate, and 0.25 μg/ml Hoechst 33258.

Cells with mating projections were prepared from midlogarithmic-phase cultures (OD_{600} = 1.2) of *MAT***a** stains grown in 5 ml of YPDA, washed twice with sterile double-distilled H_20, and incubated for 2 h in 5 ml of YPDA containing 5 μg/ml α-factor (Sigma, St. Louis, MO) before formaldehyde fixation. Spheroplasts of cells with mating projections were prepared as described above but with incubation in spheroplast solution at 37°C for only 10 min.

The distribution of filamentous actin (F-actin) was analyzed by incubating fixed cells suspended in PBS with an equal volume of rhodamine- or fluorescein isothiocyanate-conjugated phalloidin (Molecular Probes, Eugene, OR; 3.3 μM, dissolved in methanol) for 2 h at room temperature in the dark. Stained cells were washed once, resuspended in PBS, and placed onto poly(L-lysine)-coated slide for fluorescence microscopy.

Disruption of ROM2 and RHO2

Deletion of the entire open reading frames (ORFs) of the *ROM2* and *RHO2* genes was performed by the PCR-based method described by Baudin *et al.* (1993). A heterozygous *rom2Δ::HIS3/ROM2* strain (Y1241) was generated by using the primers 5′-CAGTGCTCTATTACTGCTGACTTAATTGGACAATTCATCTCTTTTCCTGCGGTTACTCTTGGCCTCCTCTAG-3′ and 5′-GTTATGCTTTTTATTCTAAAGAAAATAAGGAAAGTCTATATACGTTGCTATCGCCTCGTTCAGAATG-3′ to amplify the *HIS3* gene from pRS303. The resulting PCR product, containing the *HIS3* gene flanked on one side by 52 bp of sequence from the region directly upstream of the predicted *ROM2* initiator codon and on the other side by 47 bp of sequence

from the region directly downstream of the *ROM2* termination codon, was used to transform Y270. Transformants with correct replacement of the *ROM2* genomic locus with the *HIS3* gene were confirmed by PCR analysis and sporulated, and tetrads were dissected and analyzed.

A heterozygous *rho2Δ::TRP1/RHO2* strain (Y1693) was generated by using the primers 5′-GACATCAATTGCTGAAACGTTCTGCTTTGGTTGTGCTTTTGATCCCGTACTGGAGAGGGCCAAGAGGGAG-3′ and 5′-GTTTTTCCCTCCCTTGCTAAAAAGATAATGTATCATTTCAGTGTAAGTTTTTTGGCCTGCAGGCAAGTGCAC-3′ to amplify the *TRP1* gene from pRS304. The resulting PCR product, containing the *TRP1* gene flanked on one side by 50 bp of sequence for the region directly upstream of the *RHO2* initiator codon and on the other side by 52 bp of sequence from the region directly downstream of the *RHO2* termination codon, was used to transform Y270. Transformants were confirmed and analyzed as described above.

Identification of Multicopy Suppressors of cik1Δ^{ts}

A YEp24-based 2 μ *S. cerevisiae* genomic library (Carlson and Botstein, 1982) was transformed into a *MAT*a *cik1Δ::LEU2* strain (Y1728), spread onto plates containing synthetic complete medium lacking uracil (plasmid selection), and incubated for 12 h at the permissive temperature (room temperature) before shifting to the restrictive temperature (37°C) for 2 d. Of greater than 8000 total transformants, 34 that grew at the restrictive temperature were recovered. The plasmids from these strains were rescued into *Escherichia coli*, and 26 allowed growth at 37°C when reintroduced into Y1728 or a *cik1Δ::TRP1* strain (Y1705). Based on restriction digest analysis, these plasmids contained eight distinct sequence groups. Primers flanking the YEp24 site of genomic DNA insertion were used to generate sequence from both ends of the insert. BLAST searches with these sequences identified regions from the *S. cerevisiae* genome that were encoded by these plasmids. Subcloning techniques were then employed to identify the *cik1Δ* suppressing (*cis*) gene from each group (see summary in Table 3). In each case, plasmids containing the single ORF indicated in Table 3 were competent for suppression; control plasmids lacking the ORF failed to suppress the temperature-sensitive growth defect.

RESULTS

ROM2

ROM2 was identified in a screen for high-copy suppressors of the temperature-sensitive growth defect of a *cik1Δ* strain. Cik1p complexes with the kinesin-related microtubule motor Kar3p, and together they are required for proper chromosome segregation and karyogamy (Meluh and Rose, 1990; Page and Snyder, 1992; Page *et al.*, 1994; see below). *ROM2* is predicted to encode a 1356-amino acid protein with a region of homology to the human oncogene-encoded dbl protein (Figure 1A), a GEF for human Cdc42 (Hart *et al.*, 1991). This dbl-homology domain is common to Rho-GEFs and contains the GDP/GTP exchange activity (Hart *et al.*, 1994; Zheng *et al.*, 1994; Ozaki *et al.*, 1996). The Rom2p amino acid sequence also predicts the presence of a pleckstrin-homology domain, also common to Rho-GEFs and implicated in protein–protein or protein–phosphatidylinositol derivative interactions (Musacchio *et al.*, 1993; Lemmon *et al.*, 1996). Rom2p has recently been identified as a GEF for the yeast Rho1 protein (Ozaki *et al.*, 1996).

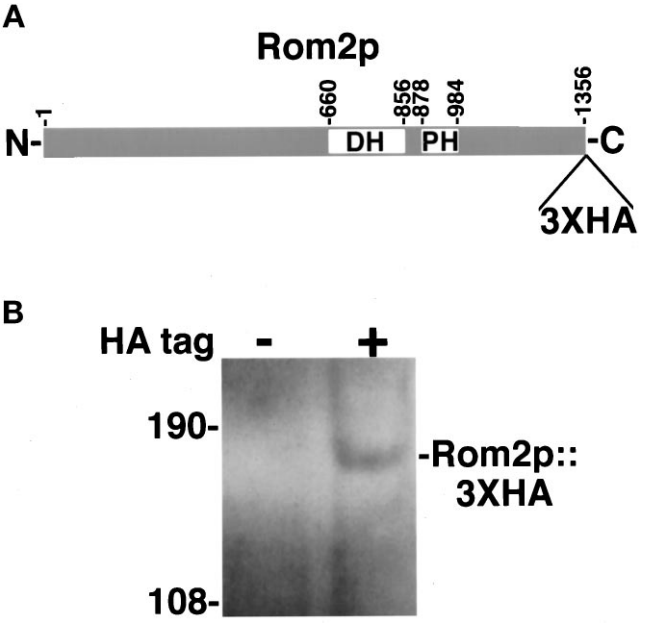

Figure 1. (A) Schematic of Rom2p. (B) Immunoblot analysis of Rom2p::3XHA. (A) The Rom2 protein is predicted to be 1356 amino acids in length and contains a dbl-homology (DH) domain from amino acids 660 to 856 and a pleckstrin homology (PH) domain from amino acids 878 to 984. Epitope tagging of the protein results in the fusion of three tandem copies of the HA epitope to the carboxyl terminus of Rom2p (see MATERIALS AND METHODS). (B) Proteins from total cell extracts of an untagged *ROM2* strain (Y1725; HA tag −) and an isogenic *ROM2::3XHA* strain (Y1723; HA tag +) were separated on an 8% polyacrylamide gel containing SDS. An immunoblot was prepared and probed with 12CA5 anti-HA monoclonal antibody (see MATERIALS AND METHODS). A protein of approximately 165 kDa is detected in extracts from *ROM2::3XHA* cells but not from *ROM2* untagged cells. The mass of molecular weight markers are shown in kilodaltons.

Rom2p Localizes to Sites of Polarized Cell Growth

To gain further insight into the function of Rom2p, we determined its subcellular localization. The genomic locus of *ROM2* was tagged with the HA epitope coding sequence (Schneider *et al.*, 1995; see MATERIALS AND METHODS). A sequence encoding three copies of the HA epitope was integrated into the carboxyl-terminal coding sequence of *ROM2*, just prior to the translational stop codon. The resulting *ROM2::3XHA* allele is functional for *ROM2* activity as growth rates at all temperatures, and bud morphology, are similar between *ROM2::3XHA* and wild-type cells (see below). Immunoblot analysis using anti-HA monoclonal antibodies detects a protein of approximately 165 kDa in cellular extracts from *ROM2::3XHA* strains but not from *ROM2* untagged strains (Figure 1B). This corresponds well to the predicted 153-kDa size of the Rom2 protein plus the triple HA epitope.

To determine the subcellular localization of the Rom2::3XHA fusion protein, indirect immunofluores-

cence using anti-HA monoclonal antibodies was performed (Pringle, *et al.*, 1991; Santos and Snyder, 1997). As shown in Figure 2, Rom2p::3XHA exhibits a cell-cycle–dependent localization pattern. The majority of unbudded cells exhibit diffuse staining throughout the cell with a few small weakly stained patches (~60% of unbudded cells, Figure 2A; total cells counted = 100). The remainder of unbudded cells contain a concentrated patch of bright staining at the cell cortex (Figure 2, B and H). Colocalization of Rom2p::3XHA and actin by using anti-HA antibodies and fluorescein isothiocyanate-conjugated phalloidin, respectively, indicates that this patch represents the presumptive site of bud emergence (our unpublished results). Rom2p::3XHA is concentrated at the bud tips of cells with emerging or small buds (>70% of tiny or small budded cells; Figure 2, C and D); some cytoplasmic patches are observed in these cells as well. In cells with larger buds, staining is more diffuse within the bud but is still concentrated toward the distal end (Figure 2E). Late in the cell cycle, when the nucleus has migrated to the bud neck (Figure 2F) and during anaphase (Figure 2G), Rom2p::3XHA localizes to cytoplasmic patches in both the mother and bud. This pattern continues through the end of mitosis and cytokinesis (Figure 2H). A strain containing Rom2p with three copies of the *myc* epitope fused to its carboxyl terminus exhibits identical cell-cycle–dependent staining patterns with anti-*myc* antibodies (our unpublished observation). Unlike F-actin and Rho1p, Rom2p::3XHA was not evident at the bud neck during cytokinesis (Adams and Pringle, 1984; Kilmartin and Adams, 1984; Yamochi *et al.*, 1994). These staining patterns were not detected in *ROM2* untagged cells at any stages of the cell cycle (Figure 2, I–L). Thus, the Rom2 protein localizes to sites of polarized bud growth, similarly to Rho1p and Cdc42p (Ziman *et al.*, 1993; Yamochi *et al.*, 1994).

Rom2p Localizes to the Tips of Mating Projections

Cdc24p is required for mating projection formation and Cdc42p localizes to the projection tip (Field and Schekman, 1980; Ziman *et al.*, 1993). As yet, the localization and function of other Rho proteins and their regulators in mating cells have not been determined. Concentration of Rom2p::3XHA at sites of vegetative polarized cell growth suggests the possibility that it may also localize to such sites in cells exposed to mating pheromone. Exponentially growing liquid cultures of *ROM2* and *ROM2::3XHA MAT***a** strains were treated with α-factor (5 μg/ml, final concentration) for 2 h and then fixed for indirect immunofluorescence analysis. Staining of *ROM2::3XHA* cells with anti-HA antibodies reveals concentration of Rom2p::3XHA at the tips of mating projections (Figure 3B, arrowheads). In addition, these cells demonstrate a diffuse or granular cytoplasmic localization of Rom2p::3XHA; the cytoplasmic staining was stronger than that observed for unbudded vegetative cells. No staining above background was detected for untagged *ROM2* cells treated with mating pheromone (Figure 3A). Therefore, Rom2p localizes to polarized cell growth sites both in vegetative and mating pheromone-treated cells.

Rom2p Is Required for Proper Cell Growth and Bud Morphology

To further understand the function of Rom2p, the entire *ROM2* genomic locus was replaced with a *HIS3* marker (see MATERIALS AND METHODS). Two independent heterozygous *rom2*Δ*::HIS3/ROM2* strains were sporulated and 20 tetrads were dissected for each. Tetrad analysis demonstrated 2:2 segregation for the *HIS* marker, and His^+ segregants grew slower at 23°C. His^+ segregants failed to grow at both 37°C and 11°C, but His^- strains were viable at both temperatures (Figure 4). Therefore, although *ROM2* is not essential at 23°C, it is required for growth at both elevated and lowered temperatures. High-copy plasmids containing either *RHO1* or *RHO2*, but not *CDC42*, suppress the temperature-sensitive growth defect of *rom2*Δ strains at 37°C (our unpublished results). This is consistent with Rom2p serving as the GEF specific for Rho1p and Rho2p, as described independently by others (Ozaki *et al.*, 1996; Schmidt *et al.*, 1997).

Cell morphology of *rom2*Δ strains was analyzed at both permissive and restrictive temperatures by using differential-interference contrast microscopy. The actin cytoskeleton was also examined in these cells by rhodamine-conjugated phalloidin staining and fluorescence microscopy (Figure 5). At the permissive temperature of 30°C, haploid *rom2*Δ strains differ in morphology from wild-type strains (four different *rom2*Δ segregants were analyzed; the results for one representative strain is quantified; Table 2). A significant number of cells (7%) with elongated buds are present (a cell with an elongated bud was scored as one in which the bud length is greater than twice the bud width, Table 2). Also, large-budded cells appear more oval or drop-shaped than those of *ROM2* strains (Figure 5B). After shifting *rom2*Δ strains to 37°C for 3 h, the proportion of cells with small buds is substantially higher than wild-type strains (49% for *rom2*Δ cells as compared with 26% for isogenic wild-type cells) and many cells with elongated buds are again observed (Figure 5D and Table 2). Cells with elongated buds are not detected at either temperature in wild-type strains. F-actin polarization in most *rom2*Δ cells resembles that of *ROM2* cells (Figure 5, A–D, rhodamine-phalloidin), in that actin patches accumulate at the incipient bud site andthroughout the bud of

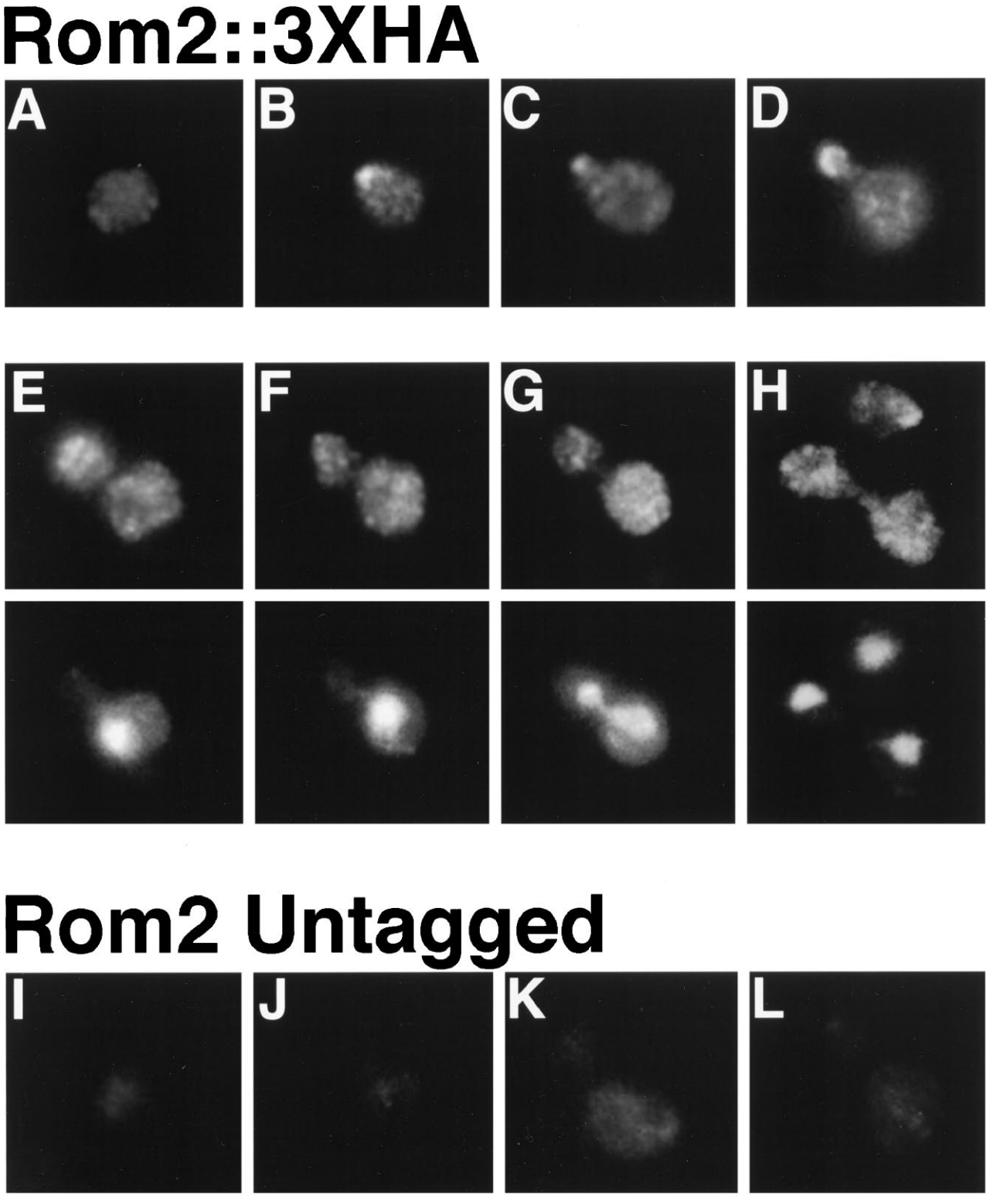

Figure 2. Cell-cycle–dependent distribution of Rom2p::3XHA. Indirect immunofluorescence with anti-HA antibodies (A–D; E–H, top; I–L) and DNA staining with Hoechst 33258 (E–H, bottom). Representative cells are pictured for a *ROM2::3XHA* strain (Y1723; A–H) and an untagged strain (Y1725; I–L). (A) An unbudded cell with diffuse cytoplasmic staining. (B) An unbudded cell with polarized cortical staining. (C) A cell with staining concentrated within an emerging bud. (D) Localization to the periphery of small buds. (E) A medium to large budded

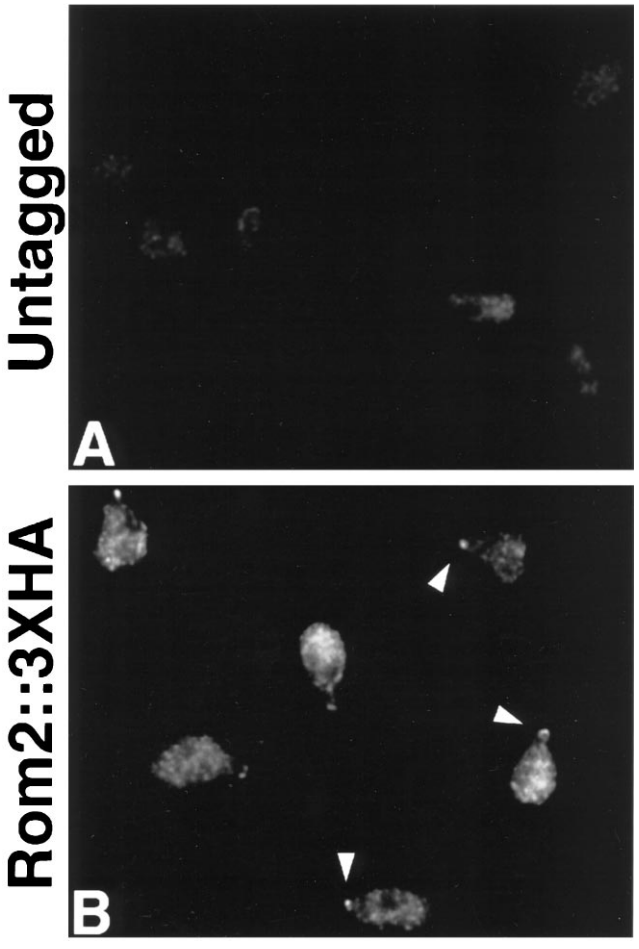

Figure 3. Mating projection localization of Rom2p::3XHA. A *MAT***a** untagged strain (Y1726; A) and a *MAT***a** *ROM2::3XHA* strain (Y1724; B) were treated with 5 μg/ml α-factor for 2 h before fixation and preparation for indirect immunofluorescence with anti-HA antibodies. Representative cells are pictured. (A) Untagged cells display very little background staining. (B) *ROM2::3XHA* cells demonstrate concentrated staining at the tips of mating projections (arrowheads) and diffuse cytoplasmic staining with some patches.

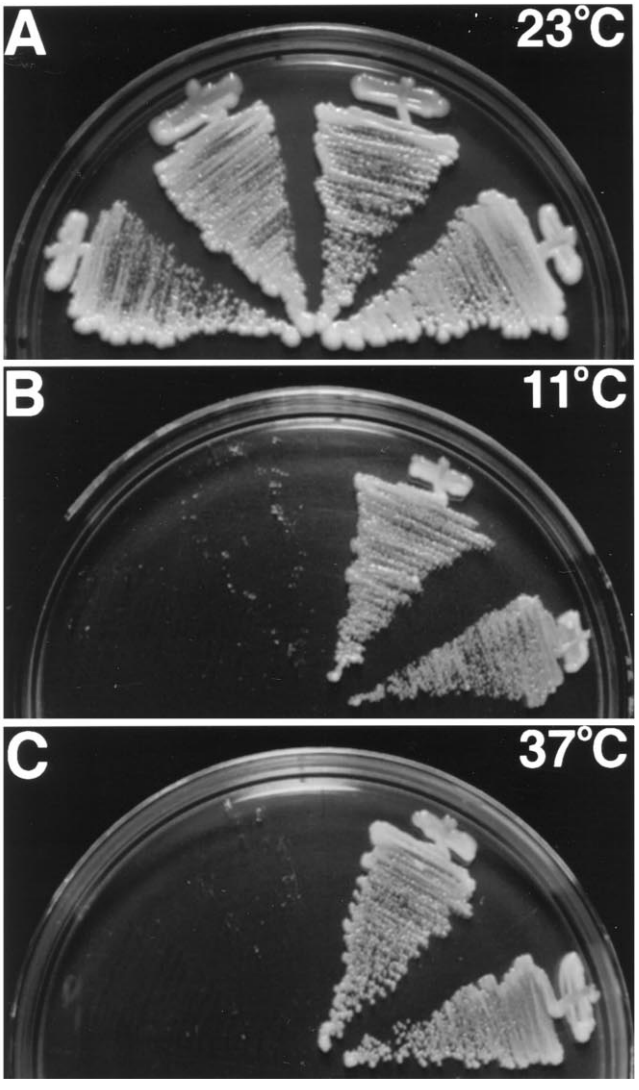

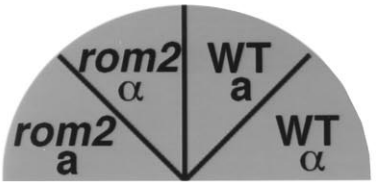

Figure 4. *rom2*Δ strains are temperature sensitive for growth at 11°C and 37°C. Haploid segregants from a *rom2*Δ*::HIS3/ROM2* heterozygous diploid (Y1241) were streaked onto plates containing YPDA medium and incubated at room temperature for 3 d (A), 11°C for 10 d (B), or 37°C for 3 d (C). Pictured are *MAT***a** *rom2*Δ (Y1245), *MAT*α *rom2*Δ (Y1242), *MAT***a** *ROM2* (Y1244), *MAT*α *ROM2* (Y1243).

small budded cells (Adams and Pringle, 1984; Kilmartin and Adams, 1984). However, in mutant cells with unusually elongated large buds, F-actin remains concentrated toward the bud tip instead of localizing throughout the bud (Figure 5B, arrowhead). At both temperatures, *rom2*Δ cells appear slightly larger than wild-type cells (Figure 5, A–D). All morphological defects of *rom2*Δ strains are suppressed by introduction of wild-type *ROM2* on a plasmid (our unpublished results). The accumulation of small-budded cells and appearance of elongated buds at the restrictive temperature are similar to the

Figure 2 (cont). cell displaying cytoplasmic patches with staining strongest toward the distal end of the bud. (F) A large budded cell with nucleus positioned at the bud neck, and (G) a large budded cell in anaphase, demonstrating cytoplasmic patch staining. (H) A cell undergoing cytokinesis with bright patch staining in the cytoplasm and an unbudded cell with polarized cortical staining. Background staining of (I) an unbudded cell, (J and K) small to medium budded cells, (L) and a large budded cell is also shown.

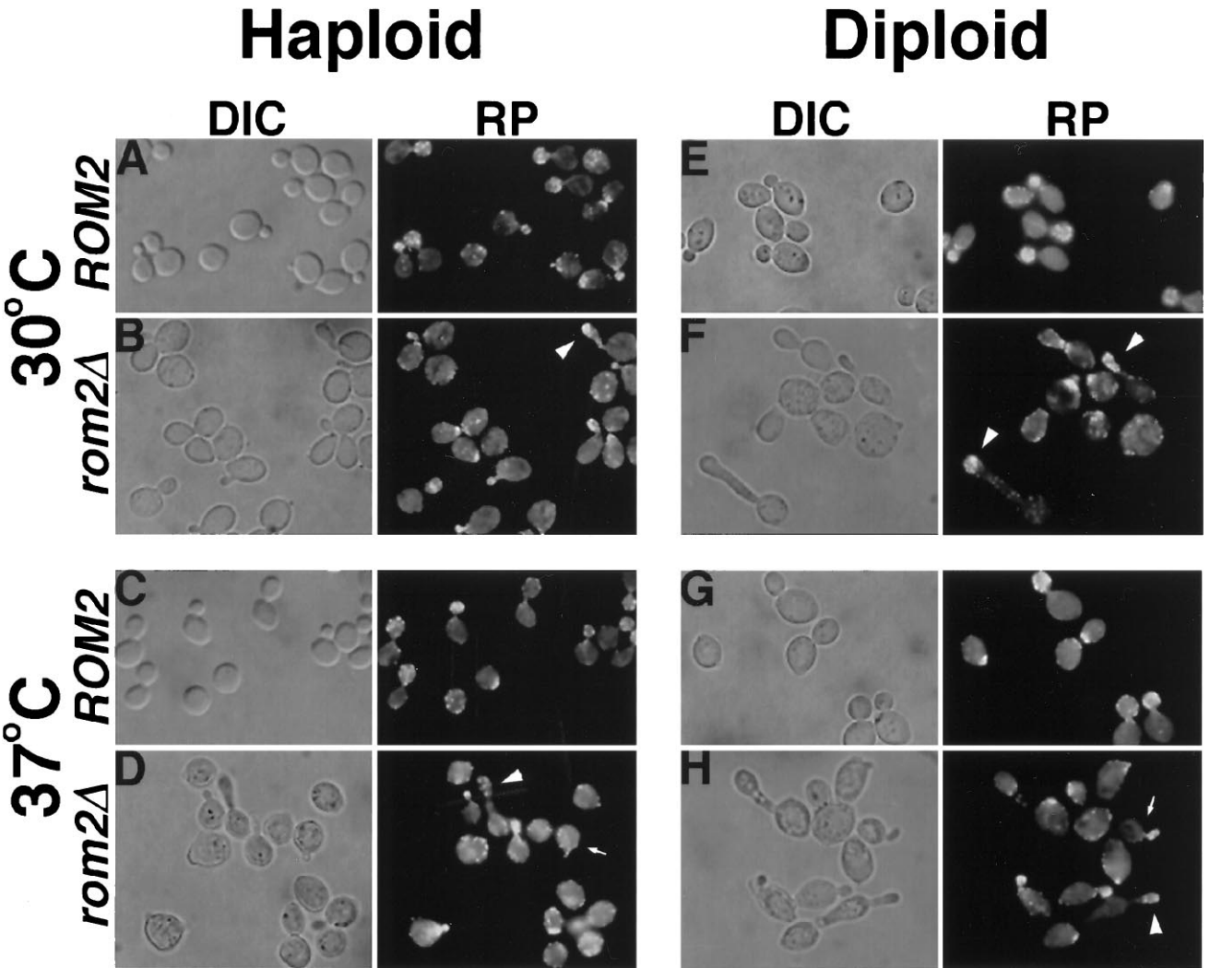

Figure 5. Morphological defects of *rom2*Δ haploids and *rom2*Δ/*rom2*Δ diploids at permissive and restrictive temperatures. Cultures of a wild-type haploid strain (Y1244; A and C), *rom2*Δ haploid strain (Y1245; B and D), wild-type diploid strain (Y270; E and G), and *rom2*Δ homozygous diploid strain (Y1241; F and H) grown at 30°C were fixed with formaldehyde (A, B, E, and F) or shifted to 37°C for 3 h before fixation (C, D, G, and H). Fixed cells were then examined by differential-interference contrast microscopy (DIC; A–H, left), and F-actin distribution was analyzed with fluorescence microscopy by staining with rhodamine-conjugated phalloidin (RP; A–H, right). Representative fields are shown. Both haploid and diploid *rom2*Δ strains exhibit cells with elongated bud morphologies at restictive and permissive temperatures (B, D, F, and H; arrowheads). Upon shift to 37°C, wild-type cells bud normally (C and G), but *rom2*Δ strains produce an increased number of small budded cells, both normal and elongated, with F-actin concentrated within the bud (D and H, arrows; see Table 2).

results of Ozaki *et al.* (1996) describing a *rom1*Δ *rom2*Δ strain containing a P_{GAL1}-*ROM2* plasmid under Rom2p-depletion conditions at 30°C. The morphological defects of *rom2*Δ strains at the permissive temperature, as well as those of the homozygous *rom2*Δ/*rom2*Δ diploid discussed below, have not been described previously.

The appearance of abnormal bud morphology is even more striking in *rom2*Δ/*rom2*Δ diploids (four homozygous diploid strains analyzed; the results for one representative strain are presented in Table 2). Approximately 30% of all budded cells at both 30°C and 37°C have elongated buds with F-actin staining concentrated toward the distal tip of the bud (Figure 5, F and H, arrowheads; Table 2). The number of small-budded cells increases upon shifting to 37°C for 3 h (46% compared with 33% for wild-type cells), but many of these are also elongated. Elongated buds are not detected for *ROM2/ROM2* wild-type diploids (Figure 5, E and G; Table 2). Chains and clusters of cells are common in *rom2*Δ/*rom2*Δ cultures, suggesting a possible defect in cytokinesis. In summary, *Rom2p* is

Table 2. Bud morphology of wild-type and *rom2*Δ strains

Strain (no. of cells)	Temperature (°C)[a]	% of total cells			% elongated[c]
		Unbudded	Small budded[b]	Medium–large budded	
Haploid					
ROM2 (309)	30	40	22	34	0
*rom2*Δ (310)	30	32	31	37	7
ROM2 (307)	37	42	26	32	0
*rom2*Δ (304)	37	27	49	24	7
Diploid					
ROM2 (318)	30	40	28	32	0
*rom2*Δ (322)	30	32	33	35	21
ROM2 (319)	37	44	33	22	0
*rom2*Δ (327)	37	25	46	29	28

[a] *ROM2* (Y1244), *rom2*Δ (Y1245), *ROM2/ROM2* (Y270), and *rom2*Δ/*rom2*Δ (Y1727) strains were grown overnight in rich medium at 30°C then fixed with formaldehyde or shifted to 37°C for 3 h before fixation.

[b] Small budded cells were scored as those with buds less than or equal to one-third the size of the mother. Medium to large budded cells were those with buds greater than one-third the size of the mother.

[c] Cells with elongated buds were scored as those whose length from neck to bud tip was greater than twice the maximum bud width. This category includes both small and large budded cells.

required to maintain proper polarized bud growth at the restrictive temperature, as evidenced by the accumulation of small-budded cells. The presence of cells with elongated buds suggests that *Rom2p* may also play a role in regulation of the switch from apical to isotropic bud growth (reviewed by Lew and Reed, 1995; see DISCUSSION).

Rom2 Is Important for Projection Formation during Mating

Mating projection formation was also analyzed in four different *rom2*Δ *MAT***a** cells. After a 2-h exposure to mating pheromone at 30°C, approximately 70% of wild-type *MAT***a** cells form mating projections of lengths greater than half the diameter of the cell (Figure 6A). In contrast, less than 20% of *rom2*Δ *MAT***a** cells under the same conditions form such projections. Mutant cells become much larger than wild-type cells and either form very small broad projections or do not form projections at all (Figure 6B). The actin cytoskeleton is polarized properly in the *rom2*Δ cells with detectable projections, as seen by rhodamine-phalloidin staining and fluorescence microscopy (our unpublished observations). Therefore, in addition to maintaining polarized cell growth during budding, Rom2p is also required for proper mating projection formation in response to pheromone.

Involvement of ROM2 in the Microtubule Cytoskeleton

We originally identified *ROM2* in a screen for high-copy suppressors of the temperature-sensitive growth defect of a *cik1*Δ strain (see MATERIALS AND METHODS; results summarized in Table 3). Interestingly, we also found *RHO2* as a *cik1* suppressing (*CIS*) gene, along with two other known loci, *MID2* and *MAT*α*-BUD5* (see Chant *et al.*, 1991; Herskowitz *et al.*, 1992),

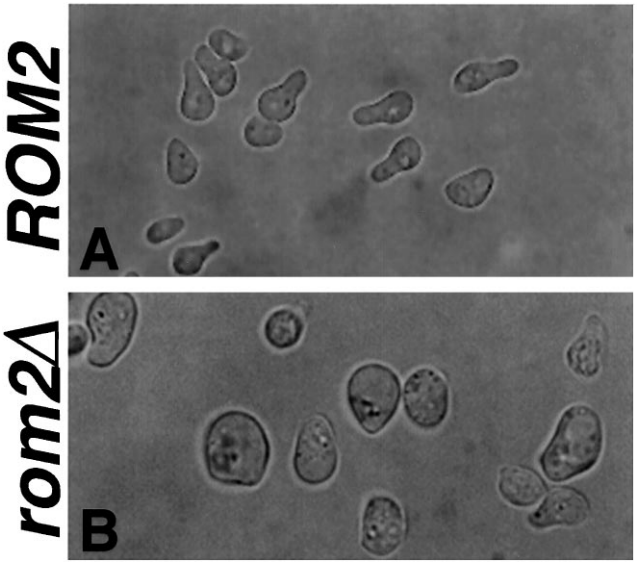

Figure 6. Mating-projection morphology defect of *rom2*Δ strains. Exponential phase cultures of a *MAT***a** *ROM2* wild-type strain (Y1244; A) and a *MAT***a** *rom2*Δ strain (Y1245; B) were treated with 5 μg/ml α-factor for 2 h, fixed, and analyzed by differential interference contrast microscopy. *ROM2* cells form normal mating projections (A), but *rom2*Δ cells become enlarged and form only short broad projections with abnormal morphology (B).

Table 3. Results of screen for 2 μ suppressors of *cik1*Δ

Suppressor (no. of isolates)	Suppression of[a] *cik1*Δ	Suppression of[a] *kar3*Δ	Identity[b]—Homology
CIS1 (1)	+	−	YDR022C—novel
CIS2 (1)	+	+	YLR299W—γ-glutamyltransferase
CIS3 (1)	+	+	YJL158C—Hsp150p homologue
CIS4 (2)	+	+	*RHO2*
CIS5 (2)	+	+	*ROM2*
CIS6 (1)	+	+	*MID2*
CIS7 (9)	+	−	*MATα,BUD5* ΔC[c]
CIS8 (9)	+	−	*CIK1*

[a]Suppression was scored by growth of *cik1*Δ (Y1705) or *kar3*Δ (Y1700) strains containing YEp24 derived plasmids with the various *CIS* genes at 37°C on solid synthetic complete medium lacking uracil (see MATERIALS AND METHODS).

[b]*Saccharomyces* Genomic Database ORF designation for previously uncharacterized genes.

[c]Suppression is specific for *cik1*Δ *MAT***a** strains; isogenic *MATα* strains containing this plasmid fail to grow at the restrictive temperature. All other *CIS* gene encoding plasmids suppress the temperature sensitivity of both *MAT***a** and *MATα cik1*Δ strains. Smallest *CIS7* plasmid tested contains the *MATα* locus and the amino-terminal end encoding two-thirds of *BUD5*. A *CEN* plasmid containing this region is sufficient for suppression.

and three previously uncharacterized genes, *CIS1*, *CIS2*, and *CIS3*. Mid2p is a transmembrane protein with a putative Ca^{2+} binding domain; *mid2*Δ mutants are sensitive to exposure to mating pheromone (Ono *et al.*, 1994). *CIS1* is predicted to encode a protein with no significant homology to known proteins. *CIS2* is predicted to encode a protein with homology to γ-glutamyltransferases from a variety of organisms (22% amino acid identity to human γ-glutamyltransferase; Sakamuro *et al.*, 1988). γ-Glutamyltransferases catalyze the transfer of glutamate residues to and from various peptide substrates, such as glutathione (Meister *et al.*, 1981); because tubulin has been shown to be posttranslationally glutamylated (Edde *et al.*, 1990), perhaps glutamylation of yeast tubulin by *CIS2* affects microtubule function. Finally, *CIS3* is predicted to encode a protein with homology to *S. cerevisiae* Hsp150p (29% amino acid identity; Russo *et al.*, 1992). Further characterization of these genes will be described elsewhere.

To determine whether the different suppressors are specific for *cik1* mutants or whether they suppress a defect resulting from loss of function of the Kar3p–Cik1p complex, we tested the ability of 2 μ plasmids containing *CIS* genes to suppress the temperature sensitivity of a *kar3*Δ strain (Table 3). *ROM2* and *RHO2* plasmids allow both *cik1*Δ and *kar3*Δ strains to grow on solid medium at the restrictive temperature of 37°C; whereas vector alone or plasmids encoding one of two other *S. cerevisiae* Rho-related proteins, Cdc42p and Rho1p, do not (Figure 7). This genetic interaction of *ROM2* and *RHO2* with a microtubule–motor complex suggests involvement of these proteins in functions of the microtubule cytoskeleton.

We analyzed whether strains lacking Rom2p or Rho2p displayed microtubule-related defects. *rom2*Δ and *rho2*Δ strains were tested for altered sensitivity to the microtubule-depolymerizing drug benomyl; failure to grow or enhanced growth in the presence of benomyl is a common characteristic of strains containing mutations in genes encoding structural or regulatory components of microtubules (e.g., Huffaker *et al.*, 1988; Hoyt *et al.*, 1991; Li and Murray, 1991; Reijo *et al.*, 1994; Pellman *et al.*, 1995; Saunders *et al.*, 1997). Wild-type *ROM2* strains grow on solid rich medium containing as much as 30 μg/ml of benomyl; in contrast, an isogenic *rom2*Δ strain fails to grow in the presence of benomyl concentrations of 20 and 30 μg/ml, and a *rho2*Δ strain displays a slight increase in benomyl sensitivity, failing to grow on plates containing 30 μg/ml (Figure 8; four mutant segregants were tested for each strain); these concentrations are similar to those that inhibit growth of several β-tubulin mutants (Reijo *et al.*, 1994). This represents the first phenotype described for a *RHO2* disruption strain. A strain containing the temperature-sensitive *rho1–104* allele has been shown previously to exhibit wild-type levels of benomyl sensitivity (Wang and Bretscher, 1995). In addition, wild-type strains containing a high-copy *ROM2* plasmid display increased resistance to benomyl compared with strains containing vector alone (the presence of the *ROM2* plasmid allows colony formation in the presence 20 μg/ml benomyl at 10^2- to 10^3-fold lower cell concentrations than cells containing vector; see MATERIALS AND METHODS; our unpublished results). Thus, phenotypic analysis supports Rom2p involvement in microtubule stability and/or function.

Interestingly, it has been reported that strains lacking Bem2p, a GAP for Rho1p and Rho2p, also display increased sensitivity to benomyl (Kim *et al.*, 1994; Wang and Bretscher, 1995; Figure 8). Because the GEF activity of Rom2p should oppose the GAP activity of Bem2p, we tested whether a *BEM2* deletion could partially suppress the growth defect of *rom2*Δ on benomyl. A double *rom2*Δ *bem2*Δ mutant was constructed by mating a *rom2*Δ*::HIS3* strain (Y1242) with a *bem2*Δ*::URA3* strain (Y930) and sporulating the resulting double heterozygous diploid. Tetrad dissection yielded His^+ Ura^- and His^- Ura^+ segregants that grew slowly as compared with His^- Ura^- wild-type segregants. His^+ Ura^+ segregants grew even slower, often taking several days to form a colony at room temperature (20 tetrads analyzed; our unpublished results). These *rom2*Δ *bem2*Δ double mutants fail to grow on the lowest concentration of benomyl tested (10 μg/ml; Figure

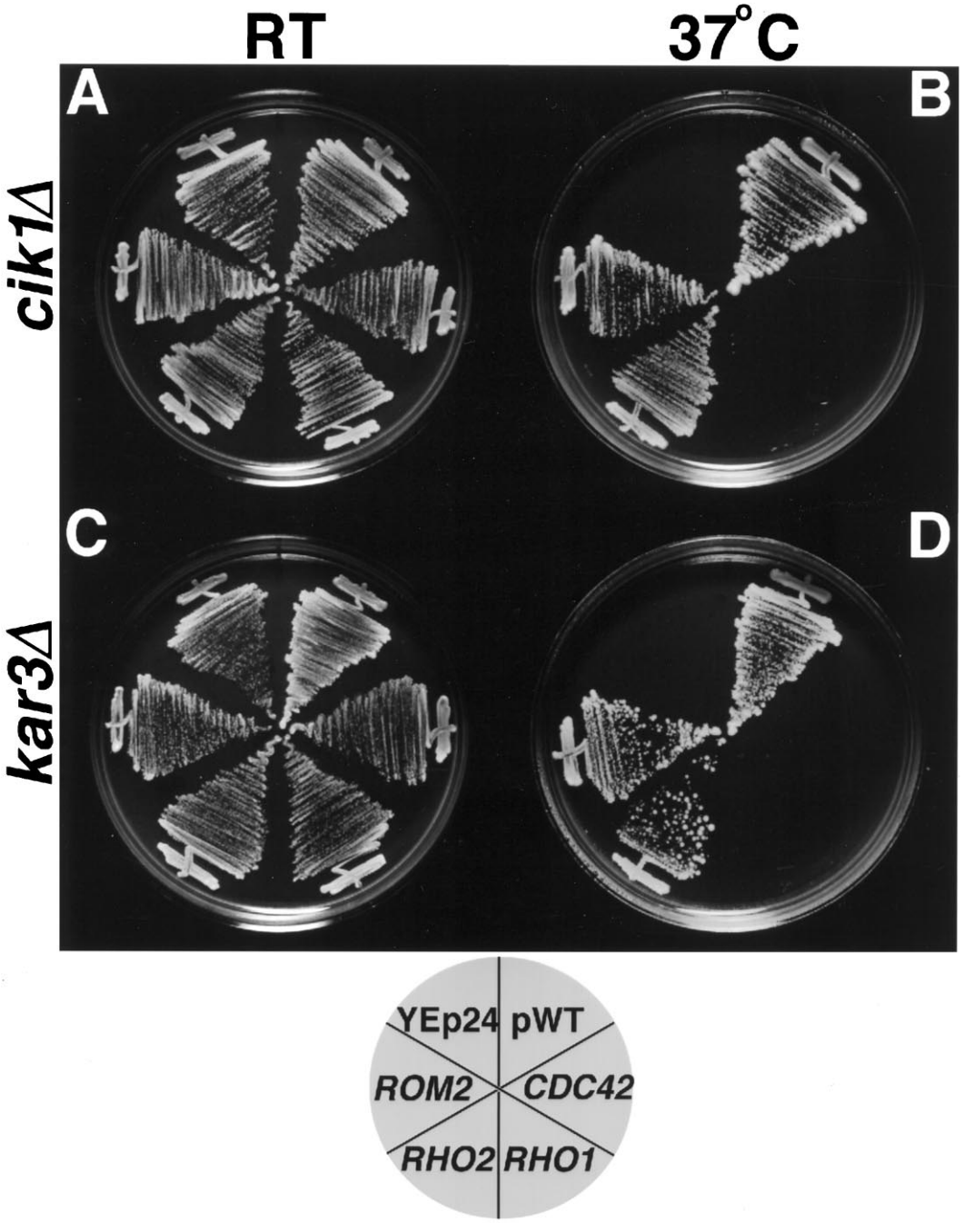

Figure 7. Increased gene dosage of *ROM2* or *RHO2* suppresses the temperature-sensitive growth defect of *cik1*Δ and *kar3* Δ strains. A *cik1*Δ strain (Y1705; A and B) or a *kar3* Δ strain (Y1700; C and D) containing YEp24-based 2 μ plasmids encoding the respective wild-type gene (pWT), *CDC42*, *RHO1*, *RHO2*, *ROM2*, or vector alone were plated to synthetic complete medium lacking uracil and incubated at either room temperature (RT; A and C) or 37°C (B and D). Strains containing *ROM2*, *RHO2*, or pWT were able to grow at the restrictive temperature of 37°C, but those containing *CDC42*, *RHO1*, or YEp24 alone failed to grow.

8; 4 His^+Ura^+ segregants tested). Therefore, disrupting both a GEF and a GAP for the Rho1p/Rho2p GTPase cycle exacerbates the defect seen in the single mutants (see DISCUSSION).

Microtubule structures from strains containing either a *ROM2* deletion or a 2 μ *ROM2* plasmid were also examined. Exponentially growing cells, as well as those from cultures treated with 5 μg/ml α-factor

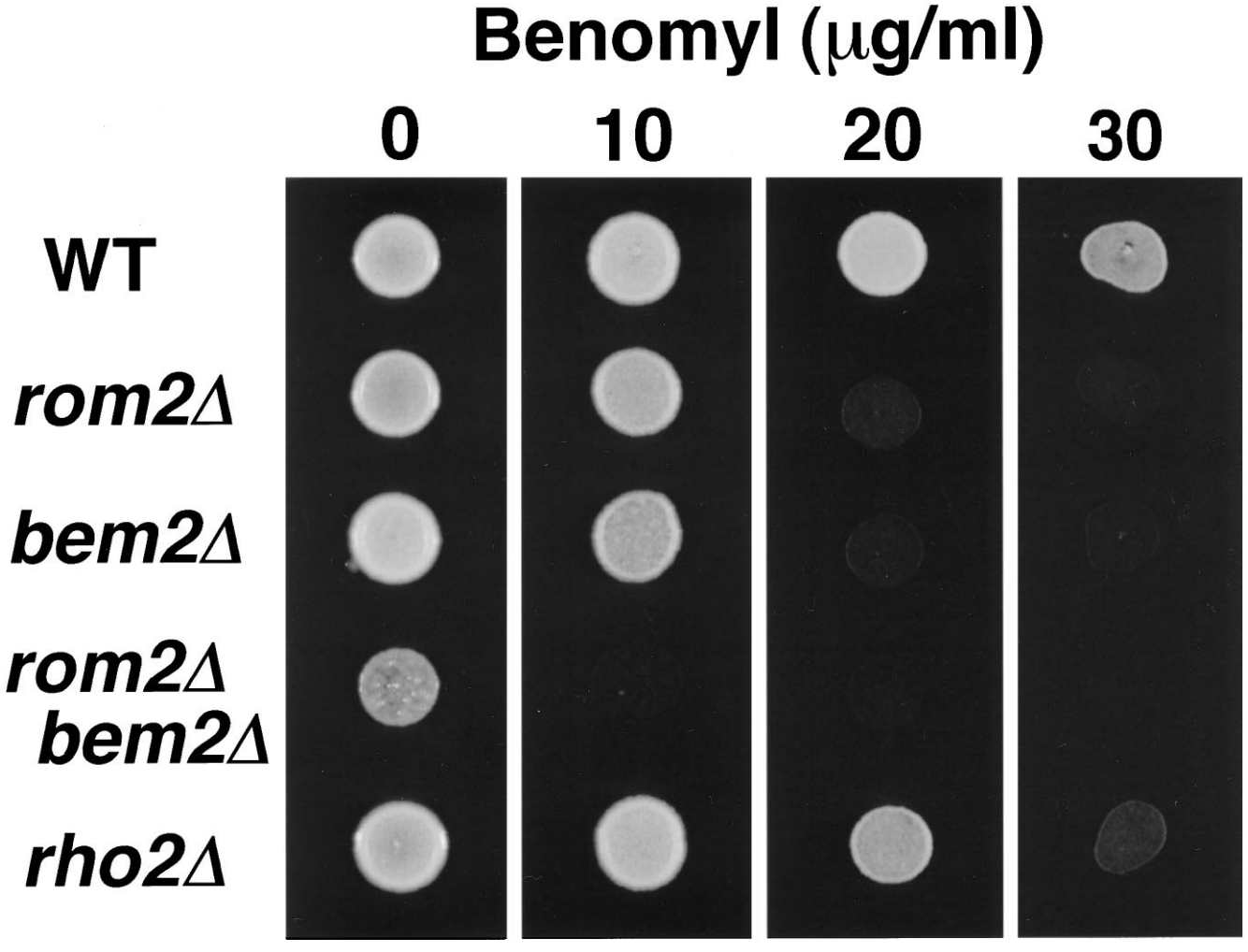

Figure 8. *rom2*Δ, *bem2*Δ, and *rho2*Δ strains exhibit increased sensitivity to benomyl. Approximately 5×10^5 cells from overnight cultures of a wild-type strain (Y1244), *rom2*Δ strain (Y1245), *bem2*Δ strain (Y930), *rom2*Δ *bem2*Δ strain (Y1709–1), and *rho2*Δ strain (Y1695) were plated in 5-μl spots to YPDA medium containing benomyl at 0, 10, 20, or 30 μg/ml. Wild-type cells grow in medium containing 30 μg/ml benomyl; cells of *rom2*Δ and *bem2*Δ mutants fail to grow in medium with 20 and 30 μg/ml benomyl; cells of a *rom2*Δ *bem2*Δ double mutant fail to grow in medium with 10 μg/ml benomyl; finally, *rho2*Δ strains are impaired for growth in medium containing 30 μg/ml benomyl.

(which arrests cells in G_1 phase) or 100 mM hydroxyurea (which arrests cells in S phase with a short spindle and the nucleus migrated to the bud neck), were analyzed by indirect immunofluorescence with anti-tubulin antibodies. No significant difference in microtubule staining pattern, length, or number was detected at any temperature compared with wild-type or vector control cells for any of the samples (our unpublished observations). Additionally, nuclear migration and spindle orientation were analyzed in the different cells by 4,6-diamidino-2-phenylindole and anti-tubulin staining, respectively. Again, no significant defect in these processes was observed (our unpublished observation). Therefore, although genetic and phenotypic analysis of *ROM2* suggests that, in addition to a role in actin-mediated events, Rom2p participates in microtubule-related functions, immunofluorescence techniques fail to detect differences in microtubule structure or cytoplasmic microtubule function (see DISCUSSION).

DISCUSSION

A Rho Regulator Localizes to Sites of Rho Activity

Despite its importance in understanding the molecular and spatial control of Rho-protein function, data on the subcellular localization of Rho regulators, in any system, have been limited. We demonstrate that the yeast Rho-GEF Rom2p localizes to sites of polarized cell growth, both during budding and mating projection formation. The cell-cycle–dependent localization

of Rom2p is very similar to that of Rho1p (Yamochi *et al.*, 1994) and represents the first example of a Rho regulator concentrating at sites of Rho function. Unlike Rom2p, another *S. cerevisiae* Rho-GEF, Cdc24p, is distributed around the entire cell periphery (Pringle *et al.*, 1995), although its target, Cdc42p, localizes to discrete sites of polarized cell growth (i.e., incipient bud sites and the tips of small buds; Ziman *et al.*, 1993). Therefore, the regulation of Cdc42p and Rho1p may differ through the spatial organization of their GEFs. One model for control of Cdc42p function is that Cdc24p is only active at sites of Cdc42p accumulation, specified by cortical cues (Pringle *et al.*, 1995). Another possibility is that Cdc24p is not regulated in a spatial manner at all; instead it may be competent for GEF activity throughout the cell periphery, and Cdc42p localization would, therefore, determine where the GTPase switch is activated.

The accumulation of both Rho1p and Rom2p at cell growth sites suggests a different mechanism for Rho1p localized activation. These proteins may localize to polarized growth sites independently by recognizing polarity establishment components, such as Cdc42p. Presumably, activation and translocation of Rom2p and release of Rho1p from cytoplasmic Rdi1p would occur at the G_1–S transition prior to bud emergence. While this manuscript was in preparation, Schmidt *et al.* (1997) found that Tor2p directly or indirectly activates the Rho1p-GEF activity of Rom2p. Perhaps the putative phosphatidylinositol kinase activity of Tor2p leads to a local accumulation of phosphatidylinositol derivatives that interact with the pleckstrin-homology domain of Rom2p (Harlan *et al.*, 1994), resulting in both polarized localization and activation of Rom2p. Rho1p may independently localize to sites of cell wall synthesis through its interaction with the transmembrane subunits of 1,3-β-glucan synthase (Qadota *et al.*, 1996). Alternatively, it is possible that Rom2p and Rho1p are interdependent for this localization or that there exists a hierarchy, perhaps with activated Rom2p responsible for recruiting Rho1p. Future localization studies should determine which of these models is correct.

Although the distributions of Rho1p and Rom2p overlap, the Rom2p::3XHA cytoplasmic patch distribution in large-budded cells and absence from the bud neck during cytokinesis differs from that reported for HA-Rho1p. In large-budded cells, HA-Rho1p staining was very faint and diffuse but reappeared at the bud neck in cells undergoing cytokinesis (Yamochi *et al.*, 1994). These differences may be due to the sensitivity of detection of each protein or could represent actual differences in the subcellular distribution of these proteins during the later stages of the cell cycle.

Rom2p Is Required for Proper Cell Growth and Polarized Morphogenesis

We have found that disruption of the *ROM2* gene in our strain background results in slow growth at room temperature and failure to grow at both 11°C and 37°C. Two independent groups have found somewhat different phenotypes for *rom2*Δ strains: Ozaki *et al.* (1996) report that along with slow growth at 20°C, these strains fail to grow at temperatures above 33°C; Schmidt *et al.* (1997) report normal growth at 37°C and impaired growth at temperatures of 30°C and lower. Presumably, these discrepancies are the result of differences in strain backgrounds.

We demonstrate that both haploid and homozygous diploid *rom2*Δ strains have various morphological defects at both restrictive and permissive temperatures. Upon shift to 37°C, *rom2*Δ strains accumulate small-budded cells with the actin cytoskeleton polarized to the bud. A strain with a temperature-sensitive allele of *RHO1* also arrests with small-budded cells and a polarized actin cytoskeleton (Yamochi *et al.*, 1994). It is likely that the cessation of bud growth observed in *rho1* and *rom2* strains at the restrictive temperature is due to loss of 1,3-β-glucan synthase activity, which has been shown to require GTP-bound Rho1p (Qadota *et al.*, 1996), and/or altered regulation of the protein kinase C signalling pathway (Drgonova *et al.*, 1996). In addition to the small-budded phenotype, many *rom2*Δ cells have elongated buds, even at the permissive temperature. The phenotype is most striking in homozygous diploid cells, with bud lengths often exceeding five times the length of its mother. This is suggestive of a defect in the switch from apical to isotropic bud growth (see Lew and Reed, 1995). It is possible that Rom2p is involved in redirecting growth from the bud tip to regions throughout the bud; regulation of Rom2p localization or function by cell cycle regulatory components might mediate this switch. Finally, although *rom2*Δ cells exposed to mating pheromone arrest normally, they become enlarged and fail to form typical wild-type mating projections. This phenotype, along with the localization of Rom2p to projection tips, demonstrates that Rom2p-mediated cellular morphogenesis extends to mating-pheromone differentiated cells as well.

Rom2p May Play a Role in Functions of the Microtubule Cytoskeleton

CIS5, a gene identified as a high-copy suppressor of the temperature-sensitive growth defect of a *cik1*Δ strain, was found to be identical to *ROM2*. Cik1p is involved in microtubule functions, such as chromosome segregation and karyogamy (Page and Snyder, 1992). Cik1p complexes with the kinesin-related Kar3 protein, a minus-end–directed microtubule motor (Meluh and Rose, 1990; Endow *et al.*, 1994; Page *et al.*,

1994). These proteins localize to spindle pole bodies and microtubules and are involved in spindle assembly and/or stability in vegetative cells (Meluh and Rose, 1990; Page *et al.*, 1994). A high-copy plasmid containing *ROM2* also suppressed a *kar3*Δ^{ts} strain, indicating that Rom2p suppresses a defect resulting from loss of the motor complex function, rather than just loss of Cik1p. Interestingly, *CIS4* was found to encode Rho2p and also suppresses the *kar3*Δ^{ts} strain. This suppression was specific for *RHO2*, as no other yeast Rho-related gene, including *RHO1*, on a 2 μ plasmid demonstrated this activity.

Similar to mutants defective in microtubule stability and/or function, *rom2*Δ strains exhibit increased sensitivity to microtubule-depolymerizing growth conditions (i.e., cold temperature and the presence of benomyl). Strains with disruptions in the *BEM2* gene also exhibit growth defects in the presence of benomyl (Kim *et al.*, 1994; Wang and Bretscher, 1995; this study). Wang and Bretscher (1995) have also observed that a *bem2*Δ strain displays synthetic lethality with a *tub2* allele defective in nuclear microtubules. Surprisingly, disruption of both *ROM2*, encoding a Rho1/Rho2-GEF (Ozaki *et al.*, 1996), and *BEM2*, encoding a Rho1/Rho2-GAP (Zheng *et al.*, 1993; Peterson *et al.*, 1994), results in an additive defect for both growth rate and benomyl sensitivity. This implies that either Rho protein cycling between GDP- and GTP-bound form is important for its function or that Rom2p and Bem2p have downstream targets of their own involved in microtubule function. Interestingly, the temperature-sensitive growth defect of *rom2*Δ was partially suppressed by disruption of *SAC7*, encoding a Rho1p-specific GAP (Schmidt *et al.*, 1997); it will be interesting to test whether *rom2*Δ *sac7*Δ double mutants also exhibit enhanced growth defects in the presence of benomyl.

There are at least two mechanisms by which Rom2p may participate in microtubule function. One possibility is that Rho proteins or their regulators affect assembly or stability of contact sites between cytoplasmic microtubules and the actin cytoskeleton. Putative microtubule-capture sites have been implicated in proper positioning of mitotic spindles prior to asymmetric cell divisions in such diverse systems as *Caenorhabditis elegans* embryogenesis and yeast budding (Hyman 1989; Snyder *et al.*, 1991; Palmer *et al.*, 1992; Cheng *et al.*, 1994). In yeast these sites are thought to lie, at least in part, at sites of polarized growth (Snyder *et al.*, 1991; Page and Snyder, 1993). However, we detected no significant difference in nuclear migration or spindle orientation in strains lacking Rom2p function. Thus, if actin–microtubule contact sites are affected in *rom2*Δ cells, it does not result in significant defects in these particular processes.

Another possibility, not mutually exclusive from the first, is that Rom2p or Rho proteins may be directly or indirectly important for microtubule stability. The differences in growth observed in *rom2*Δ strains under conditions that destablize microtubules is consistent with this possibility. In mammalian cells, it has recently been reported that Rho activation is required to stabilize wound-oriented microtubules in cultured fibroblasts and that this stabilization occurs independently of the actin cytoskeleton (Cook and Gundersen, 1996). Furthermore, it has been demonstrated that microtubule depolymerization, by treatment of fibroblasts with nocodazole, activates Rho (Liu *et al.*, 1996). The molecular basis for these events is unknown, but it is likely that they are controlled by Rho regulators, such as GEFs.

Conclusion

We have both cytologically and genetically characterized the Rho-GEF Rom2p. The localization of Rom2p to sites of Rho1p activity and the phenotypic similarities between *rho1* and *rom2* mutants provide further understanding of the mechanisms by which Rho proteins are spatially regulated. The function of Rom2p in mating-projection formation and its localization to projection tips supports evidence that components required for polarized morphogenesis are shared between the budding cycle and the mating pheromone-induced differentiation program in *S. cerevisiae* (reviewed in Madden *et al.*, 1992; Chenevert, 1994). This conservation of function may apply to polarized cell growth events in other eukaryotic systems as well. Finally, we have demonstrated genetic interactions between a Rho GTPase cycle and elements of the microtubule cytoskeleton. These and future studies should provide insight into the ever expanding functions of Rho proteins and their regulators.

ACKNOWLEDGMENTS

We thank J. Barrett, N. Burns, and S. Erdman for critical comments on the manuscript, and J. Barrett for strains and constructs. D. Johnston and Y. Takai provided the *CDC42* and *RHO1* plasmids, respectively. B.D.M. was supported by an NIH training grant. This research was supported by NIH grants GM52197 and GM36494.

REFERENCES

Adams, A., Johnson, D.I., Longnecker, R.M., Sloat, B.F., and Pringle, J.R. (1990). *CDC42* and *CDC43*, two additional genes involved in budding and the establishment of cell polarity in *Saccharomyces cerevisiae*. J. Cell Biol. *111*, 131–142.

Adams, A.E.M., and Pringle, J.R. (1984). Relationship of actin and tubulin distribution to bud growth in wild-type and morphogenetic-mutant *Saccharomyces cerevisiae*. J. Cell Biol. *98*, 934–945.

Barbet, N.C., Schneider, U., Helliwell, S.B., Stansfield, I., Tuite, M.F., and Hall, M.N. (1996). TOR controls translation initiation and early G_1 progression in yeast. Mol. Biol. Cell *7*, 25–42.

Baudin, A., Ozier-Kalogeropoulos, O., Denouel, A., Lacroute, F., and Cullin, C. (1993). A simple and efficient method for direct gene

deletion in *Saccharomyces cerevisiae*. Nucleic Acids Res. *21*, 3329–3330.

Carlson, M., and D. Botstein (1982). Two differentially regulated mRNAs with different 5′ ends encode secreted and intracellular forms of yeast invertase. Cell *28*, 145–154.

Chant, J., Corrado, K., Pringle, J.R., and Herskowitz, I. (1991). The yeast *BUD5* gene, which encodes a putative GDP-GTP exchange factor, is necessary for bud-site selection and interacts with bud-formation gene *BEM1*. Cell *65*, 1213–1224.

Chenevert, J. (1994). Cell polarization directed by extracellular cues in yeast. Mol. Biol. Cell *5*, 1169–1175.

Cheng, N., Kirby, C., and Kemphues, K. (1994). Control of cleavage spindle orientation in *Caenorhabditis elegans*: the role of the genes par-2 and par-3. Genetics *139*, 549–559.

Cook, T.A., and Gundersen, G.G. (1996). Rho regulates microtubule stability in fibroblasts. Mol. Biol. Cell *7*(suppl), 574a (Abstract).

DiComo, C.J., and Arndt, K.T. (1996). Nutrients, via the TOR proteins, stimulate the association of Tap42 with type 2A phosphatases. Genes Dev. *10*, 1904–1916.

Drgonova, J., Drgon, T., Tanaka, K., Kollar, R., Chen, G., Ford, R.A., Chan, C.S.M., Takai, Y., and Cabib, E. (1996). Rho1p, a yeast protein at the interface between cell polarization and morphogenesis. Science *272*, 277–279.

Edde, B., Rossier, J., Caer, J.L., Desbruyeres, E., Gros, F., and Denoulet, P. (1990). Posttranslational glutamylation of α-tubulin. Science *247*, 83–85.

Endow, S.A., Kang, S.J., Satterwhite, L.L., Rose, M.D., Skeen, V.P., and Salmon, E.D. (1994). Yeast Kar3 is a minus-end microtubule motor protein that destabilizes microtubules preferentially at the minus ends. EMBO J. *13*, 2708–2713.

Field, C., and Schekman, R. (1980). Localized secretion of acid phosphatase reflects the pattern of cell surface growth in *Saccharomyces cerevisiae*. J. Cell Biol. *86*, 123–128.

Fukumoto, Y., Kaibuchi, K., Hori, Y., Fujioka, H., Araki, S., Ueda, T., Kikuchi, A., and Takai, Y. (1990). Molecular cloning and characterization of a novel type of regulatory protein (GDI) for the rho proteins, ras p21-like small GTP-binding proteins. Oncogene *5*, 1321–1328.

Gehrung, S., and Snyder, M. (1990). The *SPA2* gene of *Saccharomyces cerevisiae* is important for pheromone-induced morphogenesis and efficient mating. J. Cell Biol. *111*, 1451–1464.

Guthrie, C., and Fink, G.R. (1991). Guide to yeast genetics and molecular biology. Methods Enzymol. *194*, 1–933.

Hall, A. (1994). Small GTP-binding proteins and the regulation of the actin cytoskeleton. Annu. Rev. Cell Biol. *10*, 31–54.

Harlan, J.E., Hajduk, P.J., Yoon, H.S., and Fesik, S.W. (1994). Pleckstrin homology domains bind to phosphatidylinositol-4,5-bisphosphate. Nature *371*, 168–170.

Hart, M.J., Eva, A., Evans, T., Aaronson, S.A., and Cerione, R.A. (1991). Catalysis of guanine nucleotide exchange on the *CDC42Hs* protein by the *dbl* oncogene product. Nature *354*, 311–314.

Hart, M.J., Eva, A., Zangrilli, D., Aaronson, S.A., Evans, T., Cerione, R.A., and Zheng, Y. (1994). Cellular transformation and guanine nucleotide exchange activity are catalyzed by a common domain on the *dbl* oncogene product. J. Biol. Chem. *269*, 63–65.

Herskowitz, I., Rine, J., and Strathern, J. (1992). Mating-type determination and mating-type interconversion in *Saccharomyces cerevisiae*. In: The Molecular and Cellular Biology of the Yeast *Saccharomyces*, vol II, ed. E.W. Jones, J.R. Pringle, and J.R. Broach, Cold Spring Harbor, NY: Cold Spring Harbor Laboratory Press, 583–656.

Hoyt, M.A., Toti, L., and Roberts, B.T. (1991). *S. cerevisiae* genes required for cell cycle arrest in response to loss of microtubule function. Cell *66*, 507–517.

Huffaker, T.C., Thomas, J.H., and Botstein, D. (1988). Diverse effects of β-tubulin mutations on microtubule formation and function. J. Cell Biol. *106*, 1997–2010.

Hyman, A.A. (1989). Centrosome movement in the early divisions of *Caenorhabditis elegans*: a cortical site determining centrosome position. J. Cell Biol. *109*, 1185–1193.

Imai, J., Toh-e, A., and Matsui, Y. (1996). Genetic analysis of the *Saccharomyces cerevisiae RHO3* gene, encoding a Rho-type small GTPase, provides evidence for a role in bud formation. Genetics *142*, 359–369.

Ito, H., Fukada, Y., Murata, K., and Kimura, A. (1983). Transformation of intact yeast cells with alkali cations. J. Bacteriol. *153*, 163–168.

Jacobs, C.W., Adams, A.E. M., Szaniszlo, P.J., and Pringle, J.R. (1988). Functions of microtubules in the *Saccharomyces cerevisiae* cell cycle. J. Cell Biol. *107*, 1409–1426.

Johnson, D.I., and Pringle, J.R. (1990). Molecular characterization of *CDC42* a *Saccharomyces cerevisiae* gene involved in the development of cell polarity. J. Cell Biol. *111*, 143–152.

Kilmartin, J.V., and Adams, A.E.M. (1984). Structural rearrangements of tubulin and actin during the cell cycle of the yeast *Saccharomyces*. J. Cell Biol. *98*, 922–933.

Kim, Y., Francisco, L., Chen, G., Marcotte, E., and Chan, C.S. M. (1994). Control of cellular morphogenesis by the Ipl2/Bem2 GTPase-activating protein: possible role of protein phosphorylation. J. Cell Biol. *127*, 1381–1394.

Lemmon, M.A., Ferguson, K.M., and Schlessinger, J. (1996). PH domains: diverse sequences with a common fold recruit signaling molecules to the cell surface. Cell *85*, 621–624.

Lew, D., and Reed, S. (1995). Cell cycle control of morphogenesis in budding yeast. Curr. Opin. Genet. Dev. *5*, 17–23.

Li, R., and Murray, A.W. (1991). Feedback control of mitosis in budding yeast. Cell *66*, 519–531.

Li, R., Zheng, Y., and Drubin, D. (1995). Regulation of cortical actin cytoskeleton assembly during polarized cell growth in budding yeast. J. Cell Biol. *128*, 599–615.

Liu, B.P., Chrzanowska-Wodnicka, M., and Burridge, K. (1996). Rho mediates nocodazole-induced stress fiber and focal adhesion formation. Mol. Biol. Cell *7*(suppl), 525a. (Abstract).

Madaule, P., Axel, R., and Myers, A.M. (1987). Characterization of two members of the *rho* gene family from the yeast *Saccharomyces cerevisiae*. Proc. Natl. Acad. Sci. USA *84*, 779–784.

Madden, K., Costigan, C., and Snyder, M. (1992). Cell polarity and morphogenesis in *Saccharomyces cerevisiae*. Trends Cell Biol. *2*, 22–29.

Masuda, T., Tanaka, K., Nonaka, H., Yamochi, W., Maeda, A., and Takai, Y. (1994). Molecular cloning and characterization of yeast rho GDP dissociation inhibitor. J. Biol. Chem. *269*, 19713–19718.

Matsui, Y., and Toh-e, A. (1992). Yeast *RHO3* and *RHO4* ras superfamily genes are necessary for bud growth, and their defect is suppressed by a high dose of bud formation genes *CDC42* and *BEM1*. Mol. Cell. Biol. *12*, 5690–5699.

Meister, A., Tate, S.S., and Griffith, O.W. (1981). γ-Glutamyl transpeptidase. Methods Enzymol. *77*, 237–253.

Meluh, P.B., and Rose, M.D. (1990). *KAR3*, a kinesin-related gene required for yeast nuclear fusion. Cell *60*, 1029–1941.

Musacchio, A., Gibson, T., Rice, P., Thompson, J., and Saraste, M. (1993). The PH domain: a common piece in the structural patchwork of signalling proteins. Trends Biochem. Sci. *18*, 343–348.

Novick, P., and Botstein, D. (1985). Phenotypic analysis of temperature-sensitive yeast actin mutants. Cell *40*, 405–416.

Ohga, N., Kikuchi, A., Ueda, T., Yamamoto, J., and Takai, Y. (1989). Rabbit intestine contains a protein that inhibits the dissociation of GDP from and the subsequent binding of GTP to rhoB p20, a ras p21-like GTP-binding protein. Biochem. Biophys. Res. Commun. *163*, 1523–33.

Ono, T., Suzuki, T., Anraku, Y., and Iida, H. (1994). The *MID2* gene encodes a putative integral membrane protein with a Ca^{2+}-binding domain and shows mating pheromone-stimulated expression in *Saccharomyces cerevisiae*. Gene *151*, 203–208.

Ozaki, K., Tanaka, K., Imamura, H., Hihara, T., Kameyama, T., Nonaka, H., Hirano, H., Matsuura, Y., and Takai, Y. (1996). Rom1p and Rom2p are GDP/GTP exchange proteins (GEPs) for the Rho1p small GTP binding protein in *Saccharomyces cerevisiae*. EMBO J. *15*, 2196–2207.

Page, B., and Snyder, M. (1992). CIK1: a developmentally regulated spindle pole body-associated protein important for microtubule functions in *Saccharomyces cerevisiae*. Genes Dev. *6*, 1414–1429.

Page, B., and Snyder, M. (1993). Chromosome segregation in yeast. Annu. Rev. Microbiol. *47*, 231–261.

Page, B.D., Satterwhite, L.L., Rose, M.D., and Snyder, M. (1994). Localization of the KAR3 kinesin heavy chain-like protein requires the CIK1 interacting protein. J. Cell. Biol. *124*, 507–519.

Palmer, R.E., Sullivan, D.S., Huffaker, T., and Koshland, D. (1992). Role of astral microtubules and actin in spindle orientation and migration in the budding yeast, *Saccharomyces cerevisiae*. J. Cell Biol. *119*, 583–593.

Pellman, D., Bagget, M., Tu, H., and Fink, G.R. (1995). Two microtubule-associated proteins required for anaphase spindle movement in *Saccharomyces cerevisiae*. J. Cell Biol. *130*, 1373–1385.

Peterson, J., Zheng, Y., Bender, L., Myers, A., Cerione, R., and Bender, A. (1994). Interactions between the bud emergence proteins Bem1p and Bem2p and Rho-type GTPases in yeast. J. Cell Biol. *127*, 1395–1406.

Pringle, J., Adams, A.E.M., Drubin, D.G., and Haarer, B.K. (1991). Immunofluorescence methods for yeast. In: Guide to Yeast Genetics and Molecular Biology, ed. C. Guthrie and G.R. Fink, San Diego: Academic Press, 565–601.

Pringle, J.R., Bi, E., Harkins, H.A., Zahner, J.E., Virgilio, C.D., Chant, J., Corrado, K., and Fares, H. (1995). Establishment of cell polarity in yeast. Cold Spring Harbor Symp. Quant. Biol. *60*, 729–744.

Qadota, H., Python, C.P., Inoue, S.B., Arisawa, M., Anraku, Y., Zheng, Y., Watanabe, T., Levin, D.E., and Ohya, Y. (1996). Identification of yeast Rho1 GTPase as a regulatory subunit of 1,3-β-glucan synthase. Science *272*, 279–281.

Read, E.B., Okamura, H.H., and Drubin, D.G. (1992). Actin- and tubulin-dependent functions during *Saccharomyces cerevisiae* mating projection formation. Mol. Biol. Cell *3*, 429–444.

Reijo, R.A., Cooper, E.M., Beagle, G.J., and Huffaker, T.C. (1994). Systematic mutational analysis of the yeast β-tubulin gene. Mol. Biol. Cell *5*, 29–43.

Ridley, A. (1995). Rho-related proteins: actin cytoskeleton and cell cycle. Curr. Opin. Genet. Dev. *5*, 24–30.

Russo, P., Kalkkinen, N., Sareneva, H., Paakkola, J., and Makarow, M. (1992). A heat shock gene from *Saccharomyces cerevisiae* encoding a secretory glycoprotein. Proc. Natl. Acad. Sci. USA *89*, 3671–3675.

Sakamuro, D., Yamazoe, M., Matsuda, Y., Kangawa, K., Taniguchi, N., Matsuo, H., Yoshikawa, H., and Ogasowara, N. (1988). The primary structure of human gamma-glutamyl transpeptidase. Gene *73*, 1–9.

Sambrook, J., Fritsch, E.F., and Maniatis, T. (1989). Molecular Cloning: A Laboratory Manual, 2nd ed., Plainview, NY: Cold Spring Harbor Laboratory Press.

Santos, B., and Snyder, M. (1997). Targeting of chitin synthase 3 to polarized growth sites in yeast requires Chs5p and Myo2p. J. Cell Biol. *136*, 95–110.

Saunders, W., Hornack, D., Lengyel, V., and Deng, C. (1997). The *Saccharomyces cerevisiae* kinesin-related motor Kar3p acts at preanaphase spindle poles to limit the number and length of cytoplasmic microtubules. J. Cell Biol. *137*, 417–431.

Schmidt, A., Bickle, M., Beck, T., and Hall, M.N. (1997). The yeast phosphatidylinositol kinase homolog TOR2 activates RHO1 and RHO2 via the exchange factor ROM2. Cell *88*, 531–542.

Schmidt, A., Kunz, J., and Hall, M.N. (1996). TOR2 is required for organization of the actin cytoskeleton in yeast. Proc. Natl. Acad. Sci. USA *93*, 13780–13785.

Schneider, B.L., Seufert, W., Steiner, B., Yang, Q.H., and Futcher, A.B. (1995). Use of PCR epitope tagging for protein tagging in *Saccharomyces cerevisiae*. Yeast *11*, 1265–1274.

Snyder, M., Gehrung, S., and Page, B.D. (1991). Temporal and genetic control of cell polarity in *Saccharomyces cerevisiae*. J. Cell Biol. *114*, 515–532.

Wang, T., and Bretscher, A. (1995). The rho-GAP encoded by *BEM2* regulates cytoskeletal structure in budding yeast. Mol. Biol. Cell *6*, 1011–1024.

Yamochi, W., Tanaka, K., Nonaka, H., Maeda, A., Musha, T., and Takai, Y. (1994). Growth site localization of Rho1 small GTP-binding protein and its involvement in bud formation in *Saccharomyces cerevisiae*. J. Cell Biol. *125*, 1077–1093.

Zheng, Y., Cerione, R., and Bender, A. (1994). Control of the yeast bud-site assembly GTPase Cdc42. Catalysis of guanine nucleotide exchange by Cdc24 and stimulation of GTPase activity by Bem3. J. Biol. Chem. *269*, 2369–2372.

Zheng, Y., Hart, M.J., Shinjo, K., Evans, T., Bender, A., and Cerione, R.A. (1993). Biochemical comparisons of the *Saccharomyces cerevisiae* Bem2 and Bem3 proteins. Delineation of a limit Cdc42 GTPase-activating protein domain. J. Biol. Chem. *268*, 24629–24634.

Ziman, M., Preuss, D., Mulholland, J., O'Brien, J.M., Botstein, D., and Johnson, D.I. (1993). Subcellular localization of Cdc42p, a *Saccharomyces cerevisiae* GTP-binding protein involved in the control of cell polarity. Mol. Biol. Cell *4*, 1307–1316.